Optimum fluorescence emission around 1.8 μm for $LiYF_4$ single crystals of various Tm^{3+}-doping concentrations*

Li Shan-Shan(李珊珊)[a], Xia Hai-Ping(夏海平)[a]†, Fu Li(符 立)[a], Dong Yan-Ming(董艳明)[a], Gu Xue-Mei(谷雪梅)[a], Zhang Jian-Li(章践立)[a], Wang Dong-Jie(王冬杰)[a], Zhang Yue-Pin(张约品)[a], Jiang Hao-Chuan(江浩川)[b], and Chen Bao-Jiu(陈宝玖)[c]

[a] *Key Laboratory of Photo-electronic Materials, Ningbo University, Ningbo* 315211, *China*
[b] *Ningbo Institute of Materials Technology and Engineering, Chinese Academy of Sciences, Ningbo* 315211, *China*
[c] *Department of Physics, Dalian Maritime University, Dalian* 116026, *China*

(Received 2 April 2014; revised manuscript received 20 April 2014; published online 20 August 2014)

In this paper, optical spectra of $LiYF_4$ single crystals doped with Tm^{3+} ions of various concentrations are reported. The emission intensity at 1.8 μm first increases with increasing Tm^{3+} concentration, and reaches a maximum value when the concentration of Tm^{3+} is about 1.28 mol%, then it decreases rapidly as the concentration of Tm^{3+} further increases to 3.49 mol%. The emission lifetime at 1.8 μm also shows a similar tendency to the emission intensity. The maximum lifetime of 1.8 μm is measured to be 17.68 ms for the sample doped with Tm^{3+} of 1.28 mol%. The emission cross section of $^3F_4$ level is calculated. The maximum reaches 3.76×10^{-21} cm^2 at 1909 nm. The cross relaxation ($^3H_6$, $^3H_4 \rightarrow ^3F_4$, $^3F_4$) between Tm^{3+} ions and the concentration quenching effect are mainly attributed to the change of emission with Tm^{3+} concentration. The largest quantum efficiency between Tm^{3+} ions is estimated to be ∼147% from the measured lifetime and calculated radiative lifetime. All the results suggest that the Tm^{3+}/$LiYF_4$ single crystal may have potential applications in 2 μm mid-infrared lasers.

Keywords: Tm^{3+}-doped $LiYF_4$ crystal, cross relaxation, fluorescence emission, 1.8 μm

PACS: 78.60.Lc, 78.55.Hx **DOI:** 10.1088/1674-1056/23/10/107806

1. Introduction

In recent years, the 2.0 μm solid state laser in the eye-safe region has attracted more attention due to its extensive potential applications in the fields of laser ranging, remote sensing, optoelectronic countermeasures, laser medical applications, and differential absorption lidar monitoring.[1–3] The transition $^3F_4 \rightarrow ^3H_6$ of Tm^{3+} plays an important role in generating lasers with near 2-μm radiation, and it is considered to have a key role in implementing small-scale and efficient laser sources at ∼ 2.0 μm. The quantum efficiency is likely to reach 200% due to the intense energy cross-relaxation effect ($^3H_6$, $^3H_4 \rightarrow ^3F_4$, $^3F_4$) existing between thulium ions. Such a high quantum efficiency compensates for the small Stokes efficiency of mid-infrared laser material resulting from the large energy gap between the pump and signal lasers.[4] Consequently, it is expected that Tm^{3+}-doped crystals and glasses are important candidates for ∼2-μm solid lasers. Compared with oxygen glasses and crystals as host materials, $LiYF_4$ (YLF) single crystal has low maximum phonon energy at about 425 cm^{-1}. Moreover, it also has a long lifetime of the excited electronic states in these systems compared with traditional oxide systems when it is used as a laser host. They lead to lower multiphoton emission rates, and thereby higher quantum efficiencies for mid-infrared transitions. In addition, the high chemical resistance and good thermal stability of the $LiYF_4$ single crystal make it a good matrix material. It is also proposed that relatively homogeneous concentration of Tm^{3+} in the $LiYF_4$ crystal should be able to be obtained due to the near ionic radius between Tm^{3+} (0.87 Å) and Y^{3+} (0.893 Å), which is extremely important for practical application in a laser device.

According to Dexter's model of multipolar interaction,[5] the high doping level can lead to large energy transfer rate and result in high quantum efficiency; however, it may lead to concentration quenching and reverse cross-relaxation energy transfer ($^3F_4$, $^3F_4 \rightarrow ^3H_6$, $^3H_4$), which reduces the quantum efficiency of the system.[4] Although many researchers have reported the Tm-doped $LiYF_4$,[6,7] they have just focused on one fixed doping concentration to analyze its optical properties, and no one has reported this optimum-doping concentration of the transition $^3F_4 \rightarrow ^3H_6$ in the Tm:YLF crystal. In our present experiments, $LiYF_4$ samples with different Tm^{3+}-doping concentrations (0.3, 0.5, 0.8, 1.3, 1.8, and 3.6 mol%) are fabricated, and the quantum efficiency, emission spectrum, and fluorescence decay lifetime of the $^3F_4$ manifold are characterized to find the optimum doping concentration near 1.8 μm. It is expected that this study provides a good theoretical basis for further developing and implementing near-infrared devices

*Project supported by the National Natural Science Foundation of China (Grant Nos. 51472125 and 51272109), the Natural Science Foundation of Ningbo City, China (Grant No. 201401A6105016), and K.C. Wong Magna Fund in Ningbo University, China (Grant No. NBUWC001).

†Corresponding author. E-mail: hpxcm@nbu.edu.cn

© 2014 Chinese Physical Society and IOP Publishing Ltd

around 1.8 μm.

2. Experimental procedures

The feed materials for Tm:YLF crystals were synthesized with molar compositions of 51.5 LiF–(48.5-χ) YF_3/4–χTmF_3 ($\chi = 0.3, 0.5, 0.8, 1.3, 1.8$, and 3.6 mol%). All starting materials were prepared from a stoichiometric mixture of 99.999% pure LiF, YF_3, and TmF_3 powders. In this article, a modified Bridgman process was used to grow Tm-doped YLF crystals. The mixtures were treated with anhydrous HF at 750 °C–800 °C for 8 h–10 h to ensure that feed materials were converted into polycrystalline bars; furthermore, harmful evaporation and corrosion could be minimized by sealing the crucible, thereby effectively preventing crystals from cracking. A pure $LiYF_4$ single crystal seed with the ⟨001⟩ direction was placed at the bottom of the crucible. The detailed process for crystal growth was described in Refs. [8] and [9].

A typical single crystal with a size of ϕ10 mm×77 mm that we prepared in this work is displayed in Fig. 1(c). It is transparent and pale yellow in color due to higher Tm^{3+}-dopant ion concentration, and shows that the color changed gradually from dark to light along the growth direction. The crystals were cut into small parts and well polished to 2.3 mm thickness for optical measurements. The actual concentrations of Tm^{3+} ions were measured by inductively coupled plasma atomic emission spectroscopy (ICP-AES, PerkinElmer, Optima 3000). The measured concentrations and calculated ionic concentrations are given in Table 1. The structure of the crystal was investigated by X-ray diffraction (XRD) using an XD-98X diffractometer (XD-3, Beijing). The absorption spectrum was measured with a U-4100UV/VIS/NIR spectrophotometer in a wavelength range from 400 nm to 2000 nm. The emission spectra and fluorescence decay lifetime were measured by an FLSP 920 type spectrometer (Edinburgh Co., UK) excited by an 808 nm LD. All the measurements were made at room temperature.

Table 1. Molar concentrations of Tm^{3+} in feed material and the obtained crystals, and calculated ion concentration of Tm^{3+} (N) in YLF crystals.

Feed material/mol%	0.3	0.5	0.8	1.3	1.8	3.6
Obtained crystal/mol%	0.29	0.49	0.78	1.28	1.75	3.49
$N/10^{20}$ ions/cm^3	0.73	1.22	1.95	3.17	4.46	8.79

3. Results and discussion

3.1. X-ray diffraction

The X-ray diffraction pattern of a YLF single crystal doped with Tm^{3+} (3.49 mol%) is shown in Fig. 1(b), in which the peak positions are consistent with those in JCPD 77-0816 ($a = b = 5.171$ Å, $c = 10.748$ Å) for $LiYF_4$, which is also listed in Fig. 1(a). One can deduce that the grown crystal is a single tetragonal phase and the Tm^{3+} ion dopants are introduced into crystal substitute Y^{3+} sites, so the current doping level does not cause any peak shift or other peaks. Simultaneously, the calculated cell parameters of the YLF crystal obtained in Fig. 1(b) are $a = b = 5.011$ Å and $c = 10.466$ Å, which are consistent with the fact that the radius of Tm^{3+} is less than Y^{3+}. Likewise, the efficient segregation coefficient of Tm in the $LiYF_4$ single crystal is 1.038,[10] very close to 1, suggesting that Tm^{3+} ions are well distributed and the color of the crystal is homogeneous throughout the length; this is in good agreement with what we can see from Fig. 1.

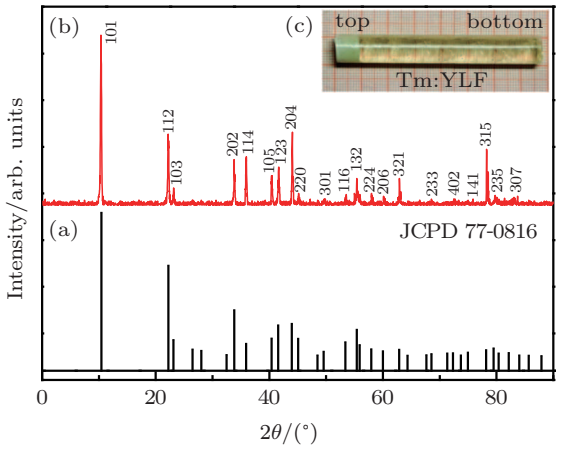


Fig. 1. (color online) (a) The standard line pattern of the tetragonal phase $LiYF_4$, (b) XRD pattern of the 3.49 mol% Tm^{3+}-doped $LiYF_4$ single crystal, and (c) photograph of Tm^{3+}-doped $LiYF_4$ single crystal.

3.2. Absorption spectra

Figure 2 shows the absorption spectra of Tm^{3+}-doped $LiYF_4$ single crystals; the corresponding energy levels are also marked in the figure. It can be seen that the absorption intensities increase dramatically with the continuous increase of the doping concentration, while the positions of the peaks do not change any more. One can conclude that the broad absorption bands in a wavelength range from 400 nm to 2000 nm can be attributed to the energy levels of Tm^{3+} ions in the same matrix.

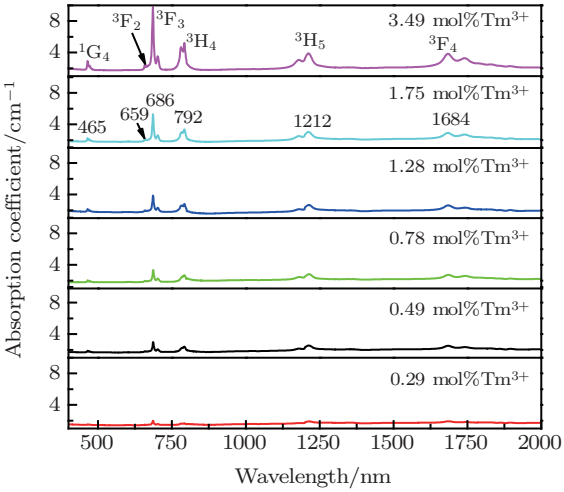


Fig. 2. (color online) Absorption spectra of various concentrations of Tm^{3+}-doped $LiYF_4$ single crystals.

Since the Tm:YLF crystals are uniaxial, in order to precisely estimate their optical properties, we measure the polarized absorption spectra with the incident light polarized parallel (π spectrum) and perpendicular (σ spectrum) to the optical axis of the samples,[11] which are shown in Fig. 3.

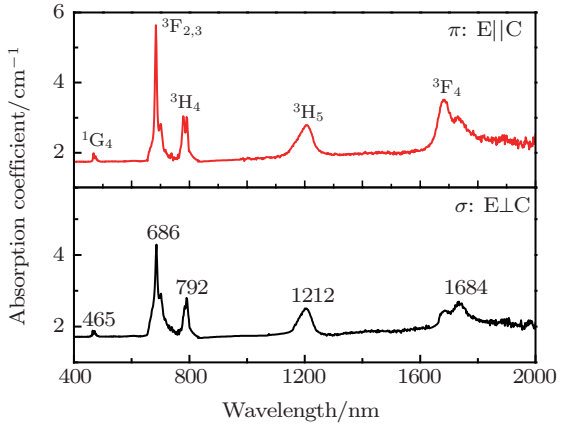


Fig. 3. (color online) Polarized absorption spectra of $LiYF_4$ single crystal doped with 1.28 mol% TmF_3.

It can be found that the polarized absorption spectra are all composed of several strong absorption bands which are consistent with absorption spectra listed in Fig. 2, from which we can see that the absorption coefficient of the π spectrum is larger than that of the σ spectrum on the whole. Based on the polarized absorption spectrum, the optical parameters of Tm^{3+} in YLF samples are obtained by applying J–O theory, which is shown to be a crucial tool for calculating and analyzing the RE-doped laser properties. To employ this method, we determine the oscillator strengths for the transitions from the $^4H_6$ states to the upper ones. The J–O intensity parameters $\Omega_{2,4,6}$ for σ and π polarizations are obtained. The effective J–O parameters $\Omega_{2,4,6}$ are given by

$$\Omega_{\text{eff}} = \frac{2\Omega_\sigma + \Omega_\pi}{3}. \tag{1}$$

The calculated values of Ω_{eff} in YLF crystals with various Tm^{3+}-doping concentrations, which are sensitive to the environment of the rare-earth ions, are listed in Table 2. It can be seen that, when the doping concentration exceeds a certain value, Ω_6 tends toward a fixed value, which indicates that the ligand field among ions is relatively constant. As an important parameter for determining the laser characteristics of a material, the radiative lifetime is defined as

$$\tau = 1/\sum_{J'} A(J \to J'), \tag{2}$$

where $A(J \to J')$ is the total transition rate between a certain state and the final J' state, the mean transition rate is determined by $A = (2A_\sigma + A_\pi)/3$, and the specific calculation details are based on Ref. [11]. Referring to Table 2, the average radiative lifetime of the $^3F_4$ manifold given by J–O theory decreases rapidly as the doping concentration changes from 0.49 mol% to 3.49 mol%.

Table 2. Intensity parameters and average radiative lifetimes of the $^3F_4$ manifold for YLF crystals doped with different Tm^{3+} concentrations, calculated from the absorption spectra (π and σ spectra).

Doping conc./mol%	$N/10^{20}$ (ions/cm^3)	$\Omega_2/10^{-20}$ cm^{-2}	$\Omega_4/10^{-20}$ cm^{-2}	$\Omega_6/10^{-20}$ cm^{-2}	τ_{rad}/ms
0.49	1.22	1.28	0.94	0.86	12.544
0.78	1.95	1.32	1.04	0.56	12.371
1.28	3.17	1.38	1.06	0.54	12.06
1.75	4.46	1.40	1.08	0.54	11.872
3.49	8.79	1.14	1.38	0.54	11.343

3.3. Fluorescence emission spectrum

Figure 4 shows the fluorescence emission spectra of Tm:YLF for various doping concentrations in a range of 1300 nm–2100 nm under excitation of an 808 nm LD. For the Tm-doped YLF crystals, there are two groups of emission peaks around 1470 nm and 1800 nm corresponding to the $^3H_4 \to {}^3F_4$ and $^3F_4 \to {}^3H_6$, respectively, which are indicated in the energy transfer mechanism of Tm^{3+} in Fig. 5. From Fig. 4, we can see that there is a broad fluorescence spectral band around 1800 nm and it is more suitable for continuous tuning and emitting a shorter pulse. As illustrated by Fig. 4, there is a very eminent effect of the Tm-doping level on fluorescence emission performance. It is noted that the fluorescence intensity at 1.8 μm constantly strengthens as Tm^{3+}-doping concentration increases from 0.29 mol% to 1.28 mol%; conversely, the fluorescence intensity at 1.47 μm declines continuously. As concentration is further increased to 1.75 mol% and 3.49 mol% separately, the corresponding fluorescence emission intensity decreases rapidly. Obviously, we can obtain the maximum fluorescence intensity at 1.8 μm. In order to see more clearly the fluorescence intensity change trend at 1800 nm, where the fluorescence spectrum extends more broadly, the relationship between the calculated normalized integral values of emission intensity from 1600 nm to 2000 nm and doping molar concentration of Tm^{3+} is inserted in Fig. 4. When the molar concentration of Tm^{3+} is 1.28 mol%, the integral value reaches a maximum, which is stronger than those for the cases of 0.78 mol% and 1.75 mol%.

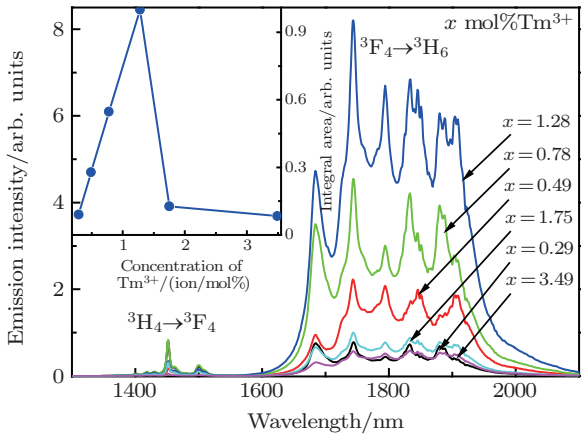


Fig. 4. (color online) Fluorescence emission spectra of Tm:YLF for various doping concentrations under the excitation of an 808 nm LD.

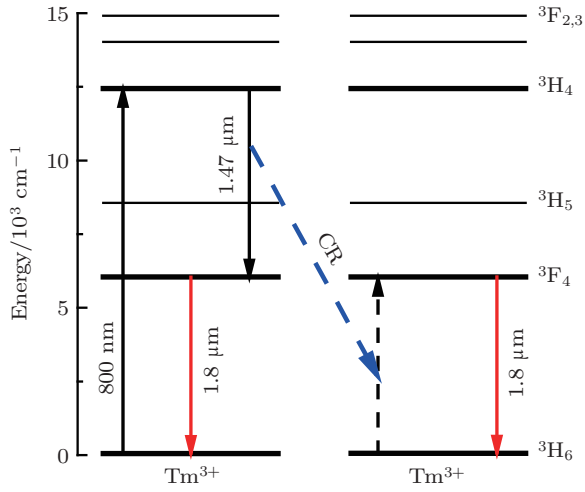


Fig. 5. (color online) Energy transfer mechanism and cross-relaxation process of Tm^{3+}.

The stronger intensity at 1.8 μm is due to the intense cross relaxation between Tm^{3+} :^{3} F_4, $^3F_4$ →^{3} H_6, $^3H_4$. Figure 5 displays the energy transfer mechanism and cross relaxation process of Tm^{3+}. As is well known, the energy gap of $^3H_4$ →$^3F_4$ is very close to that of $^3F_4$ →$^3H_6$. Pumped by an 808 nm LD, one excited Tm ion in the $^3H_4$ state decays to the $^3F_4$ manifold by transferring energy to a nearby ground state Tm^{3+}, and this ion is excited to the $^3F_4$ state as well in the meantime. As a result, two Tm ions are excited to the $^3F_4$ manifold. Hence, it is possible for the quantum efficiency of Tm^{3+} to reach 200%. Cross relaxation is closely linked to the distance between ions,[12] and this phenomenon is not obvious at lower concentrations. With increasing doping level, the distance between the ions decreases gradually and, correspondingly, the resonance transmission effect of neighboring Tm^{3+} ions occurs more strongly, thereby increasing the luminous intensity of 1.8 μm. However, when the thulium ion concentration is higher than a certain threshold, the probability of energy transfer to the quenching center increases significantly, which results in the fluorescence quenching effect. It can be seen from Fig. 4 that, when the concentration reaches 1.75 mol% (4.46×10^{20} ions/cm^3), the quenching effect can be observed markedly. After the doping level is further increased to 3.49 mol% (8.79×10^{20} ions/cm^3), the quenching effect obviously becomes stronger.

3.4. Absorption and emission cross sections

As important spectroscopic parameters for laser performance, absorption and emission cross sections are calculated. According to the measured absorption spectra, the absorption cross section (σ_{abs}) can be obtained from[13]

$$\sigma_{abs}(\lambda) = \frac{2.303\log(I_0/I)}{NL} = \frac{\alpha}{N}, \tag{3}$$

where L is the thickness of the sample, $\log(I_0/I)$ the measured optical density as a function of wavelength, N the number of Tm^{3+} ions per volume (ions/cm^3), and α the absorption coefficient.

Furthermore, the stimulated emission cross section (σ_{em}) is defined as the intensity gain of a laser beam per unit of population inversion, which is beneficial to achieving the laser effect, and it can be calculated by using the Futchbauer–Ladenburg (FL) equation given in Ref. [14]:

$$\sigma_{em}(\lambda) = \frac{\lambda^5 \cdot I(\lambda)\beta}{8\pi n^2 c\tau_{rad}\int \lambda I(\lambda)\,\mathrm{d}\lambda}, \tag{4}$$

where $I(\lambda)$ is the intensity of corrected emission spectrum, τ_{rad} the radiative lifetime calculated by J–O theory, β the fluorescence branching ratio (which is equivalent to 1 for the $^3F_4$ manifold of Tm^{3+}), λ the wavelength, c the velocity of light, and n the refractive index of the crystals.

Figure 6 exhibits absorption and emission cross sections of Tm^{3+}:$^3F_4$ manifold for 1.28 mol% and 3.49 mol% in YLF crystals. As illustrated, there is an obvious difference in emission cross section between 1.28 mol% and 3.49 mol%. It is observed that the 1.28 mol%-doped sample has strong absorption and emission intensities, and the value of emission cross section is far higher than the absorption one. There is little overlap between emission and absorption cross sections. This indicates that the emitted light has little self-absorption, producing relatively strong fluorescence output. However, for 3.49 mol% doping level, the emission intensity is much less than the absorption one; undoubtedly, the fluorescence intensity decreases rapidly. The maximum values of σ_{em} are 3.76 $\times10^{-21}$ cm^2 at 1909 nm for 1.28 mol% and 0.92 $\times10^{-21}$ cm^2 at 1909 nm for 3.49 mol%. We can therefore conclude that the 1.28 mol%-doped sample has higher cross-relaxation efficiency than the 3.49 mol% one, which is well consistent with what we have stated above in the cross-relaxation process of Tm^{3+}. The emission cross sections of various doping concentrations of the Tm^{3+}:$^3F_4$ manifold are listed in Table 3.

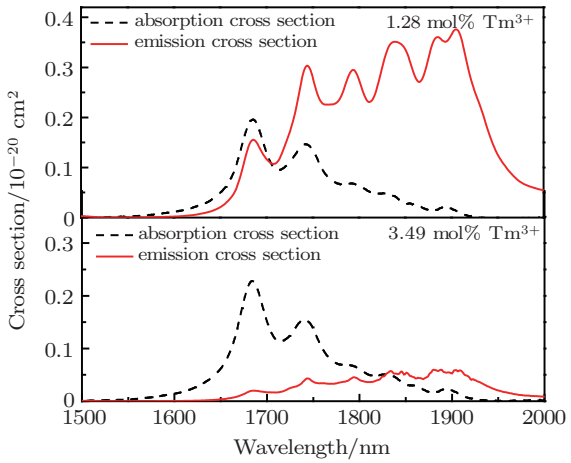


Fig. 6. (color online) Absorption and emission cross sections of Tm^{3+}:$^3F_4$ manifold in YLF crystals with Tm^{3+} at 1.28 mol% and 3.49 mol%.

3.5. Fluorescence decay curves

Under the excitation at 808 nm, the fluorescence decay curves of the $^3H_4$ multiplet at 1.8 μm for 0.49 mol%, 0.78 mol%, 1.28 mol%, 1.75 mol%, and 3.49 mol% Tm:YLF crystals are plotted in Fig. 7. The decay curves of all the Tm singly doped samples can be satisfactorily described by single exponential functions within experimental accuracy, and are also depicted in Fig. 6 in black dashed lines. The curve-fitted values (τ_{fit}) of all samples are marked in Fig. 7 for Tm-doped YLF crystals, and are very close to the values of mean lifetime (τ_m) shown in Table 3. The values of average fluorescence lifetime τ_m of the $^3F_4$ multiplet for both 0.78 mol% and 1.28 mol% are derived to be 17.66 ms and 17.68 ms. This means that stimulated ions stay in the state for a longer time and realize the population inversion more easily. The quantum efficiency η is given by the following equation:

$$\eta = \frac{\tau_m}{\tau_{rad}}, \tag{5}$$

and the values of η are 143% and 147% for 0.78 mol% and 1.28 mol%, respectively, and are listed in Table 3. Obviously, when Tm^{3+} has a higher doping density, instead, the measured lifetime and quantum efficiency decrease correspondingly. The results are attributed to the concentration quenching and reverse cross-relaxation energy transfer ($^3H_6$, $^3H_4 \rightarrow {}^3F_4$, $^3F_4$) that reduces the quantum efficiency of the system.

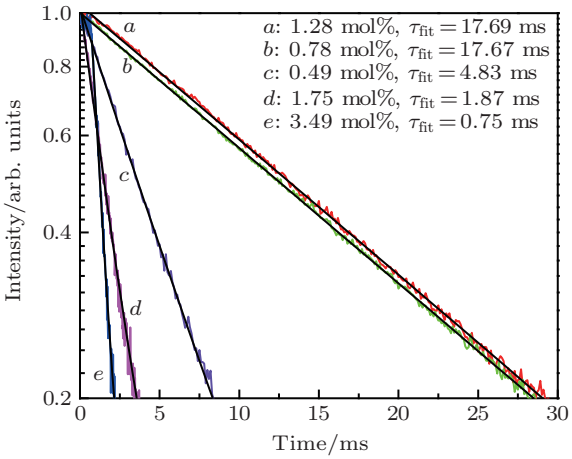


Fig. 7. (color online) Fluorescence decay curves and fitted ones for 1.8 μm of the $^3H_4$ multiplet for Tm^{3+}-doping levels of 0.49 mol%, 0.78 mol%, 1.28 mol%, 1.75 mol%, and 3.49 mol% in YLF crystals.

3.6. Gain coefficient

As a good optical gain medium for laser oscillations, the gain coefficient (G) is an important parameter, and can be obtained as follows:

$$G = N^* \times \sigma_{em}, \tag{6}$$

$$N^* = N_0 \times P \times \tau_m, \tag{7}$$

$$G \propto \sigma_{em} \times \tau_m, \tag{8}$$

where N^* is the number of the population inversion, N_0 the doping concentration of the luminous ions, and P the pumping energy density. From the above expressions, we can conclude that the gain factor is proportional to $\sigma_{em} \times \tau_m$. Table 3 displays the emission cross sections and lifetimes of the Tm^{3+}:$^3F_4$ manifold with various concentrations and some relevant research in Tm-doped YLF crystals. As shown in Table 3, of all the samples we observed in this study, the $LiYF_4$ crystal singly doped with TmF_3 at 1.28 mol% possesses the highest gain coefficient, and shows good optical characteristics in the senses of the emission cross section and fluorescence decay lifetime.

Table 3. Emission cross sections, quantum efficiencies, and lifetimes of Tm^{3+}:$^3F_4$ manifold with various concentrations in YLF crystal hosts.

Doping conc. $N/10^{20}$ cm^{-3}	$\sigma_{em}/10^{-20}$ cm^{-2}	τ_m/ms	$\sigma_{em}\tau_m/10^{-20}$ cm^2·ms	η	Ref.
1.22	0.155	4.80	0.744	0.38	This work
1.95	0.165	17.66	2.91	1.43	This work
3.17	0.376	17.68	6.65	1.47	This work
4.46	0.057	1.84	0.10	0.155	This work
8.79	0.092	0.74	0.068	0.065	This work
2.78	0.369	8.447	3.11	/	[11]
/	0.33	11.9	3.927	/	[15]

4. Conclusions

Our experiments demonstrate 1.8-μm emissions of Tm^{3+} singly doped $LiYF_4$ crystals for different doping levels of 0.49 mol%, 0.78 mol%, 1.28 mol%, 1.75 mol%, and 3.49 mol%, which are fabricated by an improved Bridgman method. A comparison of the optical spectrum among various doping concentrations is carried out. The Tm^{3+} doping concentration for 1.8-μm emission is optimized to about 1.28 mol%. At this doping level, the emission intensity at 1.8 μm reaches a maximal value because of the cross-relaxation energy transfer ($^3F_4$, $^3F_4 \rightarrow ^3H_6$, $^3H_4$) between Tm^{3+} ions, and the lifetime is 17.68 ms. The quantum efficiency of Tm^{3+} in a YLF crystal is estimated to be 147%. It is expected to be a more suitable candidate host for 2 μm continuous tuning and emitting a shorter pulse.

References

[1] Jackson S D, Sabella A and Lancaster D G 2007 *IEEE J. Sel. Topics Quantum Electron.* **13** 567

[2] Jackson S D 2009 *Laser Photon. Rev.* **3** 466

[3] Zhang Z, Shen D Y, Boyland A J, Sahu J K, Clarkson W A and Ibsen M 2008 *Opt. Lett.* **33** 2059

[4] Wu J F, Jiang S B, Luo T, Geng J H, Peyghambarian N and Barnes N P 2006 *Photon. Technol. Lett.* **18** 334

[5] Dexter D L 1953 *J. Chem. Phys.* **21** 836

[6] Razumova I, Tkachuk A, Nikitichev A and Mironov D 1995 *J. Alloys Compd.* **225** 129

[7] Pytalev D S, Klimin S A and Popova M N 2008 *Phys. Lett. A* **372** 3506

[8] Hu J X, Xia H P, Hu H Y, Zhang Y P, Jiang H C and Chen B J 2012 *J. Appl. Phys.* **112** 073518

[9] Tang L, Xia H P, Wang P Y, Peng J T, Zhang Y P, Jiang H C and Chen H B 2013 *Mater. Lett.* **104** 37

[10] Namu J, Yuan B, Ruan Y F and Yuan J 2001 *Journal of the Chinese Ceramic Society* **29** 584

[11] Xiong J, Peng H Y, Hu P C, Hang Y and Zhang L H 2010 *J. Phys. D: Appl. Phys.* **43** 185402

[12] Diestler D J, Fong F K, Freed K F, Kopelman R and Wright J C 1976 *Radiationless Processes in Molecules and Condensed Phases* (Berlin/Heidelberg: Springer) pp. 239–295

[13] Peng B and Izumitani T 1995 *Opt. Mater.* **4** 797

[14] Sokolska I, Heumann E, Kuch S and Lukasiewicz T 2000 *Appl. Phys. B* **71** 893

[15] Payne S A, Chase L L, Smith L K, Kway W L and Krupke W F 1992 *IEEE J. Quantum Electron.* **28** 2619